916 *Inorg. Chem.* **2010**, *49*, 916–923
DOI: 10.1021/ic901182c

Inorganic Chemistry
Article

FerriCast: A Macrocyclic Photocage for Fe^{3+}

Daniel P. Kennedy,[†] Christopher D. Incarvito,[‡] and Shawn C. Burdette*[,†]

[†]*Department of Chemisty, University of Connecticut, 55 North Eagleville Road U- 3060, Storrs, Connecticut 06269 and* [‡]*Department of Chemistry, Yale University, 225 Prospect Street, P.O. Box 208107, New Haven, Connecticut 06520-8107*

Received June 19, 2009

The non-siderophoric Fe^{3+} photocage FerriCast (4,5-dimethoxy-2-nitrophenyl)-[4-(1-oxa-4,10-dithia-7-aza-cyclododec-7-yl)phenyl] methanol (**2**) has been prepared in high yield using an optimized two-step reaction sequence that utilizes a trimethylsilyl trifluoromethanesulfonate (TMSOTf) assisted electrophilic aromatic substitution as the key synthetic step. Spectrophotometric assessment of Fe^{3+} binding to FerriCast revealed a binding stoichiometry and metal ion affinity dependent on the nature of the counterion. Exposure of FerriCast to 350 nm light initiates a photoreaction that converts FerriCast into FerriUnc (4,5-dimethoxy-2-nitrosophenyl)-[4-(1-oxa-4,10-dithia-7-aza-cyclododec-7-yl)phenyl]-methanone), which binds Fe^{3+} less strongly owing to resonance delocalization of the anilino lone pair into the benzophenone π-system. The release of Fe^{3+} upon photolysis of FerriCast also was evaluated using a previously reported turn-on fluorescent sensor that utilizes the same macrocyclic ligand (4-(1-oxa-4,10-dithia-7-aza-cyclododec-7-yl)phenyl, $AT_2$12C4). In contrast to the original reports on $AT_2$12C4-based Fe^{3+} sensors, FerriCast does not interact with ferric iron in aqueous solution. Introduction of oxygen containing solvents (MeOH, H_2O, DMSO, MES, and phosphate buffers) to CH_3CN solutions of metalated FerriCast lead to rapid decomplexation as measured by UV−visible spectroscopy. Further investigations contradicted the published conclusions on the aqueous coordination chemistry of $AT_2$12C4, but also confirmed the unique and unexpected selectivity of the macrocycle for Fe^{3+} in nonaqueous solvents. The crystallographic analysis of $[Cu(AT_2$12C4$)Cl]^+$ provides a rare example of a bifurcated hydrogen bond, and evidence for redox chemistry with the ligand. Spectrophotometric analysis of the model ligand with redox active metal ions provide evidence for $AT_2$12C4$^{\bullet+}$, a quasi-stable species the presence of which suggests caution should be taken when evaluating the interaction of aniline-containing systems with redox active metal ions.

Introduction

Recently, we reported on a fluorescent probe for Fe^{3+} based on the oxidation of a fluorophore pendant catechol to the corresponding quinone.[1] Fluorescent probes have the potential to help map the molecular details of biological processes related to metal ion transport, homeostasis, and participation in disease pathology.[2] Similarly, caged complexes have been used to understand such processes by using light to introduce well-defined concentrations of metal ions into systems with temporal and spatial control.[3] We also reported on new methodologies for preparing nitrobenzhydrol-based caged complexes for divalent metal ions using an aza-crown ether ligand as a chelator.[4] With our interests in iron sensors, caged complexes, and macrocyclic ligands, we were intrigued by the report of a fluorescent sensor (**3**) for ferric iron that utilizes a unique *N*-phenyl-1-oxa-4,10-dithia-7-azacyclododecane ($AT_2$12C4, **1**) macrocycle as the receptor (Figure 1).[5] This article has been cited frequently since it is a rare example of a turn-on sensor for Fe^{3+} that utilizes a photoinduced electron transfer (PeT) signaling mechanism. The report is significant since the macrocycle is reported to be not only highly selective for ferric iron but also the key component of a sensor that exhibits an enhancement of emission, which is unusual fluorescence behavior with redox active metal ions. Iron is ubiquitous in biology, so sensors and caged complexes have the potential to elucidate important functions and consequences of free iron.

Intuitively, the $AT_2$12C4 macrocycle would not be predicted to possess Fe^{3+} selectivity since it utilizes two soft thioether ligands and an ethereal oxygen to bind a hard Lewis

*To whom correspondence should be addressed. E-mail: shawn.burdette@uconn.edu.

(1) Kennedy, D. P.; Kormos, C. M.; Burdette, S. C. *J. Am. Chem. Soc.* **2009**, *131*, 8578–8586.
(2) Que, E. L.; Domaille, D. W.; Chang, C. J. *Chem. Rev.* **2008**, *108*, 4328–4328.
(3) Ellis-Davies, G. C. R. *Chem. Rev.* **2008**, *108*, 1603–1613.
(4) Kennedy, D. P.; Gwizdala, C.; Burdette, S. C. *Org. Lett.* **2009**, *11*, 2587–2590.
(5) Bricks, J. L.; Kovalchuk, A.; Trieflinger, C.; Nofz, M.; Bueschel, M.; Tolmachev, A. I.; Daub, J.; Rurack, K. *J. Am. Chem. Soc.* **2005**, *127*, 13522–13529.

Published on Web 01/04/2010

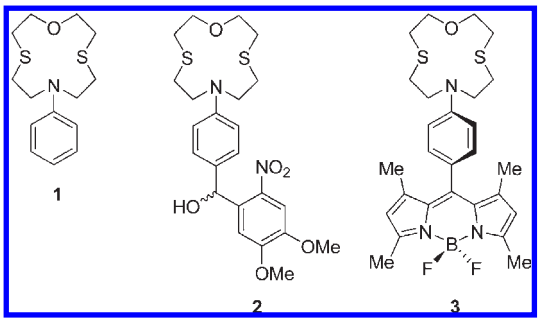

Figure 1. Structures of compounds containing the $AT_2$12C4 macrocycle.

acid. Instead of hard−soft acid base interactions dominating binding, the ligand's selectivity derives from the size of the cavity,[6] which exactly matches the small diameter of Fe^{3+} (0.63 Å).[7] Of other common transition metal ions, only Cu^{2+} has a significant affinity for the macrocycle; however, it binds more weakly since Cu^{2+} has a slightly larger diameter (0.71 Å) than Fe^{3+}.[7] The $AT_2$12C4 ligand has also been used as a receptor for Ag^+ in a fluorescent ionically driven molecular IMPLICATION gate, but the authors state in a footnote that this receptor is better suited for Fe^{3+} and Cu^{2+}.[8] Additionally, the parent macrocycle has been utilized as a Cu^+ receptor in a photoresponsive azobenzene that bind O_2,[9] a Ag^+ receptor in inorganic polymeric networks,[10] a Zn^{2+} or Cu^{2+} receptor in ferrocenyl derived redox chemosensors,[11] and a Hg^{2+} receptor in a dansyl-derived turn-off fluorescent sensor.[12] We envisioned using this unique chelator to make a caged complex for Fe^{3+} that would complement our existing fluorescent probe. The original article reported that sensors utilizing $AT_2$12C4 bound Fe^{3+} in aqueous solution at pH 5;[5] however, when the related (**2**) failed to reproduce this binding in water, we decided to investigate the coordination chemistry of $AT_2$12C4 more thoroughly.

Experimental Section

General Synthetic Procedures. All the materials listed below were of a research grade or a spectro-grade in the highest purity commercially available from Acros Organics or TCI America. Dichloromethane (CH_2Cl_2), toluene ($C_6H_5CH_3$) and tetrahydrofuran (THF) were sparged with argon and dried by passage through a Seca Solvent Purification System. All chromatography and TLC were performed on silica (230−400 mesh) from Silicycle unless otherwise specified. Activated basic alumina (∼150 mesh) was obtained from Acros Organics. TLCs were developed with mixtures of ethyl acetate (EtOAc)/hexanes unless otherwise specified and were visualized with 254 and 365 nm light and I_2 vapor. ^{1}H and ^{13}C NMR spectra were recorded using a Bruker 300 MHz NMR instrument, and chemical shifts are reported in parts per million on the δ scale relative to tetramethylsilane. IR spectra were recorded on a Nicolet 205 FT-IR instrument, and the samples were prepared as KBr pellets. High resolution mass spectra were recorded at the University of Connecticut mass spectrometry facility using a micromass Q-Tof-2 mass spectrometer operating in positive ion mode. The instrument was calibrated with Glu-fibrinopeptide B 10 pmol/μL using a 50:50 solution of acetonitrile (CH_3CN) and H_2O with 0.1% acetic acid (AcOH). *N*,*N*-bis-(2-bromoethyl) aniline was synthesized according to literature procedures.[13] The fluorescent sensor **3** was prepared as described.[5]

7-Phenyl-1-oxa-4,10-dithia-7-aza-cyclododecane (1). Sodium metal (825 mg, 35.9 mmol) was added to iPrOH (200 mL) and refluxed for 3 h. The resulting solution was cooled to room temperature and 2,2′-dimercaptoethyl ether (2.25 g, 16.3 mmol) was added. The solution was bought to reflux, and a solution of *N*,*N*-bis-(2-bromoethyl) aniline (5.00 g, 16.3 mmol) in iPrOH (125 mL) was added dropwise over 1 h. The mixture became heterogeneous within 30 min. The mixture was refluxed for 16 h, cooled to room temperature, and the solvent removed. The crude residue was adsorbed onto 20 mL of silica, and purification by flash chromatography (20:3 petroleum ether/EtOAc) afforded the product as a white powder (2.2 g, 50%). Recrystallization from toluene/petroleum ether afforded **1** as colorless, columnar prisms. TLC R_f = 0.34 (silica, 20:3 petroleum ether/EtOAc). Mp = 106−108 °C. ^{1}H NMR (300 MHz, $CDCl_3$) δ 7.26 (2 H, m, phenyl H); 6.71 (3 H, m, phenyl H); 3.80 (8 H, m, CH_2); 2.95 (4 H, t, J = 7.1 Hz, CH_2's); 2.85 (4 H, t, J = 4.6 Hz, CH_2's). ^{13}C NMR (75 MHz, $CDCl_3$) δ 147.8, 129.5, 115.9, 111.2, 73.7, 50.3, 32.3, 30.7 ppm. IR (KBr) 3060−3024, 2949−2788, 1596, 1504 cm^{-1}. HRMS (+ESI) Calcd for MH^+ 284.1143; Found, 284.1140.

(4,5-Dimethoxy-2-nitrophenyl)-[4-(1-oxa-4,10-dithia-7-aza-cyclododec-7-yl)phenyl] methanol (FerriCast, 2). Ortho-nitroveratraldehyde (323 mg, 1.30 mmol) and 2,6-lutidine (178 μL, 1.54 mmol) were added sequentially to a solution of **1** (283 mg, 1.00 mmol) in CH_2Cl_2 (100 mL). TMSOTf (236 μL, 1.30 mmol) was added to the resulting solution dropwise. After stirring for 1 h of at 23 °C, an additional portion of 2,6-lutidine (178 μL, 1.54 mmol) and TMSOTf (236 μL, 1.30 mmol) was added to the solution. An identical aliquot of 2,6-lutidine and TMSOTf was added after an additional 1 h of reaction time. TBAF (7.0 mL, 1 M in THF) was added to the reaction mixture, and the solution was stirred for 5 min. The combined organic mixture was washed with saturated brine, dried over excess anhydrous Na_2SO_4, and the solvent was removed. Flash chromatography on silica (5:3 hexanes/EtOAc) afforded FerriCast (**2**) as an amorphous orange foam (377 mg, 76.2%). TLC R_f = 0.31 (silica, 5:3 hexanes:EtOAc). ^{1}H NMR (300 MHz, $CDCl_3$) δ 7.62 (1 H, s, phenyl H); 7.45 (1 H, s, phenyl H); 7.15 (2 H, AA′XX′, phenyl H); 6.58 (2 H, AA′XX′, phenyl H); 6.47 (1 H, d, J = 3.0 Hz, methine H); 4.00 (3 H, s, methyl H); 3.95 (3 H, s, methyl H); 3.74 (8 H, m, CH_2); 2.88 (4 H, t, J = 6.83 Hz, CH_2); 2.81 (4H, t, J = 4.30 Hz, CH_2); 2.54 (1 H, d, J = 3.5 Hz, OH). ^{13}C NMR (75 MHz, $CDCl_3$) δ 153.3, 147.7, 147.5, 140.0, 134.8, 129.4, 128.4, 111.0, 110.1, 108.1, 73.6, 71.3, 56.4, 56.3, 50.2, 32.3, 30.7 ppm. IR (KBr) 3430, 3101, 2918−2793, 1613, 1520 (ν_{asym} NO_2), 1333 (ν_{sym} NO_2) cm^{-1}. HRMS (+ESI) Calcd for MH^+ 495.1624; Found, 495.1583.

(4,5-Dimethoxy-2-nitrosophenyl)-[4-(1-oxa-4,10-dithia-7-aza-cyclododec-7-yl)phenyl]-methanone (FerriUnc, 4). FerriCast (47 mg, 95 μmol) was dissolved in CH_3CN (3.0 mL) and placed into a quartz cuvette. The resulting bright yellow solution was irradiated for 5 h with a 1000 W Xe lamp. The resulting dark orange colored solution was evaporated to dryness, and flash chromatography on basic alumina (1:1 EtOAc/hexanes) afforded FerriUnc (**4**) as an orange, amorphous foam (20 mg, 42%). TLC R_f = 0.17 (basic

(6) Niu, C.-R.; Jiang, H.; Wu, C.-T.; Luo, B.-S. *Chem. Res. Chin. Univ.* **1998**, *14*, 375–378.
(7) Shannon, R. D. *Acta Crystallogr., Sect. A* **1976**, *A32*, 751–767.
(8) Rurack, K.; Trieflinger, C.; Koval'chuck, A.; Daub, J. *Chem.—Eur. J.* **2007**, *13*, 8998–9003.
(9) Shinkai, S.; Shigematsu, K.; Honda, Y.; Manabe, O. *Bull. Chem. Soc. Jpn.* **1984**, *57*, 2879–84.
(10) Tei, L.; Blake, A. J.; Cooke, P. A.; Caltagirone, C.; Demartin, F.; Lippolis, V.; Morale, F.; Wilson, C.; Schroeder, M. *Dalton Trans.* **2002**, 1662–1670.
(11) Caltagirone, C.; Bencini, A.; Demartin, F.; Devillanova, F. A.; Garau, A.; Isaia, F.; Lippolis, V.; Mariani, P.; Papke, U.; Tei, L.; Verani, G. *Dalton Trans.* **2003**, 901–909.
(12) Aragoni, M. C.; Arca, M.; Bencini, A.; Blake, A. J.; Caltagirone, C.; Decortes, A.; Demartin, F.; Devillanova, F. A.; Faggi, E.; Dolci, L. S.; Garau, A.; Isaia, F.; Lippolis, V.; Prodi, L.; Wilson, C.; Valtancoli, B.; Zaccheroni, N. *Dalton Trans.* **2005**, 2994–3004.
(13) Chang, E. Y. C.; Price, C. C. *J. Am. Chem. Soc.* **1961**, *83*, 4650–4656.

alumina, 1:1 EtOAc:hexanes). ^{1}H NMR (400 MHz, $CDCl_3$) δ 7.75 (2 H, AA′XX′, phenyl H); 7.14 (1 H, s, phenyl H); 6.59 (2 H, AA′XX′, phenyl H); 6.34 (1 H, s, phenyl H); 4.05 (3 H, s, OCH_3); 3.92 (3 H, s, OCH_3); 3.86 (4 H, t, J = 5.2 Hz, CH_2); 3.76 (4 H, t, J = 3.4 Hz, CH_2); 2.87 (4 H, t, J = 5.2 Hz, CH_2), 2.83 (4 H, t, J = 3.4 Hz, CH_2). ^{13}C NMR (100 MHz, $CDCl_3$) δ 193.8, 160.0, 156.0, 152.1, 150.1, 140.2, 133.0, 127.0, 110.3, 110.0, 91.9, 76.9, 73.6, 57.0, 56.4, 50.5, 33.1, 31.1 ppm. IR (KBr) 3091, 2918, 2856, 2794, 1645 (ν_{CO}), 1591 (ν_{NO}) cm^{-1}. HRMS (+ESI) Calcd MNa^+ 499.1337; Found, 499.1315.

General Spectroscopic Methods. All solutions were prepared with spectrophotometric grade solvents. Absorption spectra were recorded on a Cary 50 UV−visible spectrophotometer under the control of a Pentium IV-based PC running the manufacturer supplied software package. Spectra were routinely acquired at 25 °C, in 1 cm path length quartz cuvettes with a total volume of 3.0 mL. Fluorescence spectra were recorded on a Hitachi F-4500 spectrophotometer under the control of a Pentium-IV PC running the FL Solutions 2.0 software package. Excitation was provided by a 150 W Xe lamp (Ushio Inc.) operating at a current of 5 A. Spectra were routinely acquired at 25 °C, in 1 cm quartz cuvette with a total volume of 3.0 mL using, unless otherwise stated, 5 nm slit widths and a photomultiplier tube power of 700 V.

Titrations of FerriCast and Fluorescent Sensor 3 with $FeCl_3$, $Fe(ClO_4)_3$, and HCl. Stock solutions of the ligands and metal salts were prepared at μM−mM concentrations in spectrophotometric grade CH_3CN (J.T. Baker). The commercially available metal salts (Strem and EM Science) were of the highest purity available and used as is. A standardized solution of 1.00 M HCl was used to prepare a 4.03 mM aqueous stock solution. To assess the fluorescence response of sensor **3** to Fe^{3+} or H^+ the excitation wavelength was set at λ_{ex} = 470 nm, and unless otherwise stated, the total concentration of the ligand was 1.0 μM. To assess the binding stoichiometry of FerriCast and **3** with Fe^{3+} the method of continuous variation was performed in triplicate with both the perchlorate and the chloride salt. To acquire absorbance spectra for solutions containing between 0.0 and 100 μM Fe^{3+}, the method of reciprocal dilutions was used. The spectrum of a 3000 μL CH_3CN solution of 100 μM ligand was recorded. To prepare a solution containing 10 μM Fe^{3+} and 90 μM ligand in the first iteration (n = 1), 300 μL of the ligand solution was removed from the cuvette and replaced with 300 μL of stock 100 μM Fe^{3+}, and the absorbance spectrum was recorded. The process was repeated for n = 2−9 iterations by removing from the cuvette and replacing with [1/(11 − n) × 3000] μL of stock Fe^{3+}. Difference spectra for n = 1−9 were calculated from $Abs_n - Abs_{Lig} \times \chi_{Lig} - Abs_{Fe} \times \chi_{Fe}$, where Abs_n is the absorbance spectrum for the nth iteration, Abs_{Lig} is the absorbance spectrum of ligand alone, χ_{Lig} is the mole fraction of ligand, Abs_{Fe} is the absorbance of Fe^{3+} alone, and χ_{Fe} is the mole fraction of Fe^{3+}. The resulting difference in absorbance was plotted as a function of wavelength. Job's plots were prepared using absorbance data of the electronic transition that occurs at 272 nm. Solutions of FerriCast and **3** (25 μM for absorbance measurements and 1.0 μM for fluorescence measurements, λ_{ex} = 470 nm) were titrated with stock solutions of $FeCl_3$ and $Fe(ClO_4)_3$ in CH_3CN. All titrations were performed in triplicate for FerriCast and only once for **3**. The conditional binding constants with $Fe(ClO_4)_3$ (log β_{12}) and with $FeCl_3$ (log β_{11} and log β_{12}) were found by fitting the data with the least-squares fitting program HypSpec.[14,15] The values for the binding constants found for each trial were averaged, and a standard deviation was calculated. Binding of FerriUnc to $FeCl_3$ was assessed by titrating a 20 μM solution of the ligand in CH_3CN. The conditional dissociation constant (K_d') was calculated by fitting the data at 350 nm with a 1:1 binding isotherm:

$$\Delta Abs_{350} = \frac{C_{tot}\Delta\varepsilon[Fe^{3+}]}{K_d' + [Fe^{3+}]} \quad (1)$$

where ΔAbs_{350} is $|Abs_{measured} - Abs_{ligand} - Abs_{Fe(III)}|$, C_{tot} is 20 μM, $\Delta\varepsilon$ is $\varepsilon_{complex} - \varepsilon_{ligand} - \varepsilon_{Fe}$, K_d' is the dissociation constant for complex FeL^{3+}, and $[Fe^{3+}]$ is the concentration of uncomplexed Fe^{3+}. The three values for K_d' found for each cation were averaged, and a standard deviation was calculated.

Complex Stability to O-Containing Solvent Systems. Solutions of fully formed 1:2 $Fe(ClO_4)_3$/ligand complexes (25 μM FerriCast and **3**) were prepared in CH_3CN and then titrated with DMSO, CH_3OH, deionized H_2O, 10 mM MES buffer pH = 5.8 and 10 mM phosphate buffer pH = 2.2. The extent of decomplexation was assessed spectrophotometrically by measuring the restoration of the absorbance of *apo*-FerriCast at 272 nm and *apo*-**3** at 266 nm. The percentage of decomplexation was calculated from the following formula;

$$\%\text{Decomplexation} = \frac{Abs_{measured} \times \frac{V_0 - V_{add}}{V_0} - Abs_{complex}}{Abs_{ligand} - Abs_{complex}} \times 100 \quad (2)$$

where $Abs_{measured}$ is the measured absorbance at the analytical wavelength, $Abs_{complex}$ and Abs_{ligand} are the absorbance of the fully formed complex and free ligand at the analytical wavelength, respectively, the volume of added solvent is given as V_{add}, and the initial volume of the solution containing fully formed complex is V_0. The point at which half of the complex remained in solution (50% decomplexation) is defined as DC_{50} and was assessed graphically and reported as a volume percent (V/V) of the oxygen-containing co-solvent.

Quantum Yields of Photolysis. The intensity of the 150 W Xe source was found by irradiating a 5 mM aqueous solution of $K_3[Fe(oxalate)_3]$ at λ = 420 nm. A 100 μL aliquot of the irradiated solution was added after 5 min intervals to 3000 μL of a fresh 15 mM aqueous solution of ferrozine, a colorimetric probe for Fe^{2+} (λ_{max} = 562 nm/ε = 27900 cm^{-1} M^{-1}),[16] in a 1 cm quartz cuvette and the concentration of the Fe^{2+} formed (mol cm^{-3}) was found by the following formula:

$$\frac{3100\,\mu\text{ L} \quad Abs_{562} \quad 1\text{ L}}{100\,\mu\text{ L}\ 27900\text{ mol}^{-1}\text{ L}\ 1000\text{ cm}^3} \quad (3)$$

The intensity of the source (I) was then calculated using the reported quantum yield of photolysis for $K_3[Fe(oxalate)_3]$ (Φ = 1.21)[17] and the following formula;

$$I = \frac{\frac{\Delta[Fe^{2+}]}{\Delta\text{time}}}{\Phi_{photolysis}} N_A \quad (4)$$

where N_A is Avogadro's number (6.022×10^{23}) and Δtime at 300, 600, and 900 s. The intensities calculated for each three time points were averaged, and a standard deviation was calculated. A typical result was I = 1.3 (±0.3) × 10^{14} quanta sec^{-1} cm^{-3}.

A 25 μM solution of FerriCast in CH_3CN in a 1 cm quartz cuvette was irradiated at 350 nm, and absorbance spectra were recorded at 5, 15, 30, 45, 60, 90, 120 min intervals. The concentration of the photoproduct FerriUnc (mol cm^{-3}) was

(14) Gans, P.; Sabatini, A.; Vacca, A. *Talanta* **1996**, *43*, 1739–1753.
(15) Gans, P.; Sabatini, A.; Vacca, A. *Ann. Chim.* (*Rome*) **1999**, *89*, 45–49.
(16) Stookey, L. L. *Anal. Chem.* **1970**, *42*, 779–781.
(17) Hatchard, C. G.; Parker, C. A. *Proc. R. Soc. London, Ser. A* **1956**, *235*, 518–536.

Table 1. Crystallographic Parameters for [Cu(AT$_2$12C4)Cl](CuCl$_2$)

formula	$Cu_2Cl_3S_2ONC_{14}H_{21}$
formula wt	516.90
space group	$P\bar{1}$ (#2)
a, Å	8.60035(18)
b, Å	10.2079(2)
c, Å	12.2655(3)
α, deg	66.5117(14)
β, deg	79.6174(15)
γ, deg	81.6212(15)
V, Å^3	968.15(4)
Z	2
ρ_{calcd} (g cm^{-3})	1.773
absorp. coeff. (cm^{-1})	85.391
temp, K	93
total no. data	13221
no. unique data	3250
obs data[a]	3250
no. parameters	209
R, %[b]	0.0480
*wR*2, %[c]	0.0950
max/min peaks, e/Å	0.77, −0.51

[a] Observation criterion: $I > 2\sigma(I)$. [b] $R = \sum||F_o| - |F_c||/\sum|F_o|$. [c] $wR2 = [\sum w(F_o^2 - F_c^2)^2/\sum w(F_o^2)^2]^{1/2}$.

calculated at 350 nm with the following equation;

$$[\text{FerriUnc}] = \frac{A_{350} - 5700\ \text{M}^{-1}\ C_{tot}}{39300\ \text{M}^{-1} - 5700\ \text{M}^{-1}} \frac{1\ \text{L}}{1000\ \text{cm}^3} \quad (5)$$

where C_{tot} is 25 × 10^{-6} M and the molar absorptivities of FerriCast and FerriUnc at 350 nm are 5700 cm^{-1} M^{-1} and 39300 cm^{-1} M^{-1}, respectively. The quantum yield of photolysis was calculated using an equation similar to 4;

$$\Phi_{photolysis} = \frac{\frac{\Delta[\text{FerriUnc}]}{\Delta\text{time}}}{I} N_A \quad (6)$$

The values calculated at each time interval were averaged, and a standard deviation was calculated. The experiment was repeated in the presence of 25 μM (1.0 equiv) $FeCl_3$ and 1.0 μM (0.04 equiv) **3** where FerriCast is saturated but binding to the photoproduct FerriUnc is negligible. All photolysis experiments were duplicated.

Collection and Reduction of X-ray Data. Structural analysis was carried out in the X-ray Crystallographic Facility at Yale University. Crystals were covered with oil, and a green prism of $Cu_2Cl_3S_2ONC_{14}H_{21}$ with approximate dimensions of 0.20 × 0.20 × 0.20 mm was mounted on a glass fiber at room temperature and transferred to a Rigaku RAXIS RAPID imaging plate area detector with graphite monochromated Cu Kα radiation (λ = 1.54187 Å) controlled by a PC running the Rigaku CrystalClear software package.[18] The data were collected at a temperature of −180 ± 1 °C to a maximum 2θ value of 136.5°. The data were corrected for Lorentz and polarization effects. The structure was solved by direct methods[19] and expanded using Fourier techniques.[20] The space group was determined by examining systematic absences and confirmed by the successful solution and refinement of the structure. The non-hydrogen atoms were refined anisotropically. Hydrogen atoms were refined using the riding model. All calculations were performed using the CrystalStructure[21] crystallographic software package except for refinement, which was performed using SHELXL-97.[19] Relevant crystallographic information is summarized in Table 1 and Table 2, and the 50% thermal ellipsoid plot is shown in Figure 2.

Table 2. Selected Interatomic Distances (Å) and Angles (deg) for [Cu(AT$_2$12C4)Cl](CuCl$_2$)[a]

bond lengths		bond angles	
Cu(1)−Cl(1)	2.2167(13)	Cl(1)−Cu(1)−S(2)	93.41(4)
Cu(2)−Cl(2)	2.1021(12)	Cl(1)−Cu(1)−S(1)	93.47(4)
Cu(2)−Cl(3)	2.1143(11)	S(1)−Cu(1)−N(1)	88.72(8)
Cu(1)−N(1)	2.036(3)	N(1)−Cu(1)−S(2)	88.55(8)
Cu(1)−O(1)	2.255(2)	Cl(1)−Cu(1)−O(1)	98.53(8)
Cu(1)−S(1)	2.3596(9)	O(1)−Cu(1)−N(1)	98.98(10)
Cu(1)−S(2)	2.3638(9)	S(2)−Cu(1)−O(1)	83.60(6)
		O(1)−Cu(1)−S(1)	82.77(6)
		Cl(2)−Cu(2)−Cl(3)	176.91(6)
		Cl(1)−Cu(1)−N(1)	162.49(7)
		S(1)−Cu(1)−S(2)	165.50(3)

[a] Number in parentheses are estimated standard deviations in the last digit(s). Atom labels are provided in Figure 2.

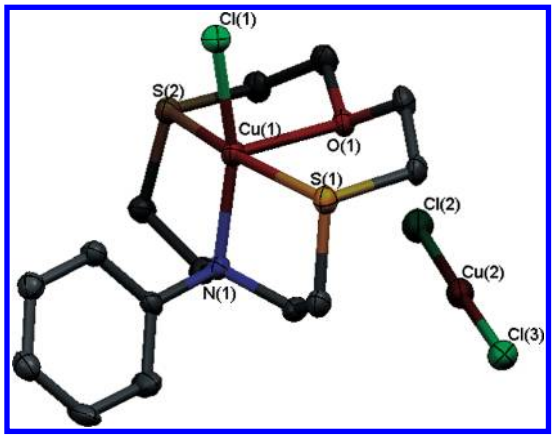

Figure 2. ORTEP diagram of FerriCast model complex [Cu(AT$_2$-12C4)Cl](CuCl$_2$) showing 50% thermal ellipsoids and selected atom labels. Hydrogen atoms are omitted for clarity.

Results and Discussion

Synthesis. The desired ligand FerriCast (**2**) was prepared in high yield from **1** and ortho-nitroveratraldehyde using the trimethylsilyl trifluoromethanesulfonate (TMSOTf) promoted electrophilic aromatic substitution reaction pioneered by Tsien (Scheme 1).[22] Our new cross coupling methods[4] were not screened for synthesizing this cage because sulfur compounds usually poison Pd catalysts. By modifying the standard reaction conditions,[22] the overall yield of the desired compound was increased from 23% to 76%. These changes included running the reaction dilute (0.01 M instead of 0.2 M), replacing 2,6-di-*t*-butyl pyridine with 2,6-lutidine, and adding TMSOTf and 2,6-lutidine in three separate portions over the course of 3 h. The modifications prevent the formation of malachite green-like byproducts,[23] which are observed when the reaction is carried out under the originally reported conditions. Removal of the TMS group with tetrabutylammonium fluoride (TBAF) in situ provided the caged macrocycle. The name FerriCast is derived

(18) *CrystalClear and CrystalStructure*; Rigaku/MSC: The Woodlands, TX, 2005.
(19) Sheldrick, G. M. *SHELX97*; Bruker AXS: Madison, WI, 1997.
(20) Beurskens, P. T.; Admiraal, G.; Beurskens, G.; Bosman, W. P.; de Gelder, R.; Israel, R.; Smits, J. M. M. *DIRDIF99*; University of Nijmegen: The Netherlands, 1999.
(21) *CrystalStructure 3.8: Crystal Structure Analysis Package*; Rigaku and Rigaku Americas: The Woodlands, TX, 2007.
(22) Adams, S. R.; Kao, J. P. Y.; Grynkiewicz, G.; Minta, A.; Tsien, R. Y. *J. Am. Chem. Soc.* **1988**, *110*, 3212–3220.
(23) Schweizer, F.; Muehlethaler, B. *Farbe Lack* **1968**, *74*, 1159–1173.

Scheme 1. Synthesis of FerriCast and FerriUnc

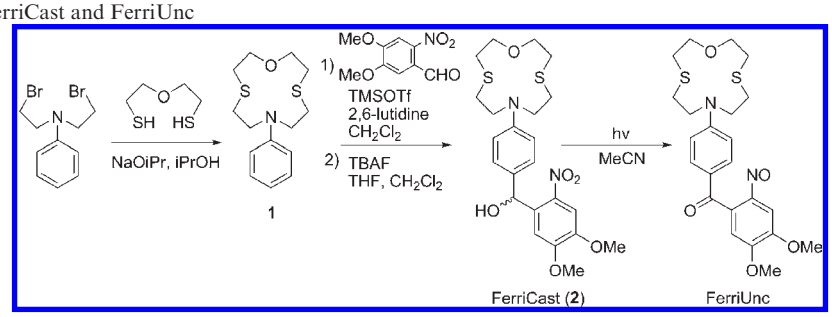

from the selectivity of the ligand for *ferric* iron and the ability to *cast* off the metal ion upon photolysis.

Photochemistry. To demonstrate the uncaging efficiency, FerriCast was complexed with Fe^{3+} in CH_3CN and photolyzed to the corresponding nitrosoketone FerriUnc (Figure 3). The name FerriUnc refers to the *uncaged* form of the ligand. Isolation and characterization of the photoproduct facilitates the determination of binding constants and quantum yields of photolysis without interference from the unphotolyzed cage. FerriCast acts as a ferric iron cage in CH_3CN. Photolysis of the 25 μM complex in the presence of 1.0 μM **3** at 350 nm with a 150 W source resulted in the dramatic increase in the fluorescence emission (Figure 3). Fluorescence enhancements observed during the photolysis are indicative of the formation of $[Fe(\mathbf{3})]^{3+}$ because of reduced binding affinity of FerriUnc for Fe^{3+}. Upon formation of the nitrosobenzophenone, the aniline-lone pair in the macrocyclic receptor becomes delocalized by resonance, which significantly reduces the ability of the receptor to bind Fe^{3+}. The quantum yield of photolysis of apo-FerriCast (ε_{350} = 5700 cm^{-1} M^{-1}, $\Phi = 1.0 \pm 0.1\%$) and the complex (ε_{350} = 11,890 cm^{-1} M^{-1}, $\Phi = 4.0 \pm 1.2\%$) are in accord with nitrobenzhydrol derived caged complexes.[22,24] The major limitation in using low intensity illumination is the sluggish rate of photolysis that result in half-lives of hours. Typically caged complexes are employed in biological investigations using either flash lamp or laser flash photolysis. Flash techniques expose samples to a high number of photons on very short time scales.[25] Future studies with FerriCast and related cages will utilize flash photolysis to better demonstrate the efficacy of using these cages for biological applications.

Metal Binding Properties. The binding of FerriCast to $Fe(ClO_4)_3$ initially was assessed by UV−vis spectroscopy in CH_3CN (Figure 4). Addition of the perchlorate salt to a solution of the ligand led to the erosion of an aniline derived electronic transition at ~270 nm (Figure 4). Job analysis of the spectral changes reveal the presence of a tightly bound 1:2 M/L complex (Figure 5). When FerriCast was titrated with $Fe(ClO_4)_3$, the spectroscopic changes fit to a 1:2 binding isotherm with a calculated binding constant of log β_{12} = 13.2 ± 0.2. When the experiments were repeated in aqueous solution at any pH, no Fe^{3+}-binding was observed.

When the perchlorate groups were replaced by chloride anions, Job's analysis provided ambiguous information about the stoichiometry, which can be indicative of ill-defined complexes in solution.[26,27] Titration data with $FeCl_3$ modeled with the linear least-squares fitting program HypSpec[14,15,28] is suggestive of two complexes in solution with binding constants log β_{11} = 5.5 ± 0.1 and log β_{12} = 8.4 ± 0.1. Simulations with Hyss[28] using the calculated binding constants for the 1:1 and 2:1 complexes with chloride anions reveal that the 2:1 species

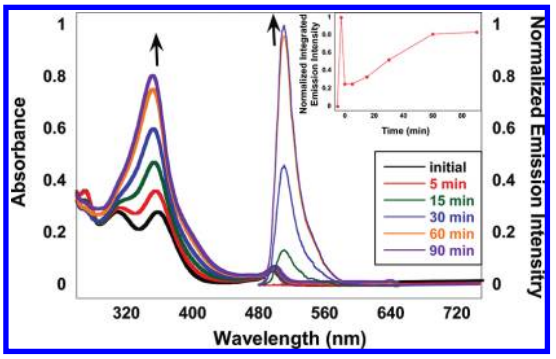

Figure 3. Changes observed in FerriCast absorption (bold lines) and sensor **3** emission (thin lines) of 25 μM $[Fe(FerriCast)_2]Cl_3$ and 1.0 μM **3** in CH_3CN upon photolysis (λ_{ex} = 350 nm, 150 W Xe source). Inset: Changes in integrated emission with time. Prior to photolysis the emission of **3** was measured before and after the addition of Fe^{3+}. The decrease in emission at t = 0 corresponds to the addition of excess FerriCast to the metalated sensor.

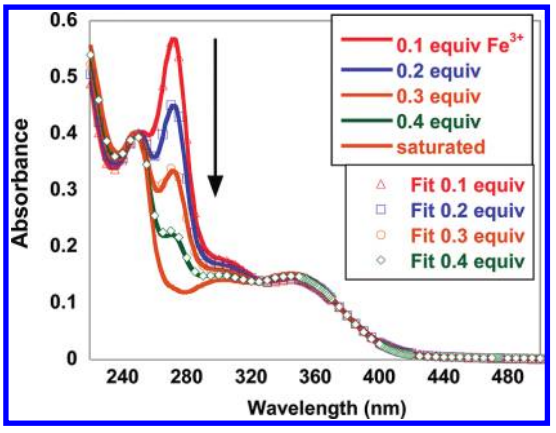

Figure 4. Titration of 25 μM FerriCast in CH_3CN with $Fe(ClO_4)_3$. The open circles represent the fit obtained from the program HypSpec. The ligand saturates at about 0.5 eq of Fe^{3+}. The arrow indicates erosion of the band at 270 nm upon addition of Fe^{3+}.

(24) Ellis-Davies, G. C. R. *Cell Calcium* **2006**, *39*, 471–473.
(25) Rapp, G. *Methods Enzymol.* **1998**, *291*, 202–222.
(26) Vosburgh, W. C.; Cooper, G. R. *J. Am. Chem. Soc.* **1941**, *63*, 437–442.
(27) Atkinson, G. F. *J. Chem. Educ.* **1974**, *51*, 792–798.
(28) Alderighi, L.; Gans, P.; Ienco, A.; Peters, D.; Sabatini, A.; Vacca, A. *Coord. Chem. Rev.* **1999**, *184*, 311–318.

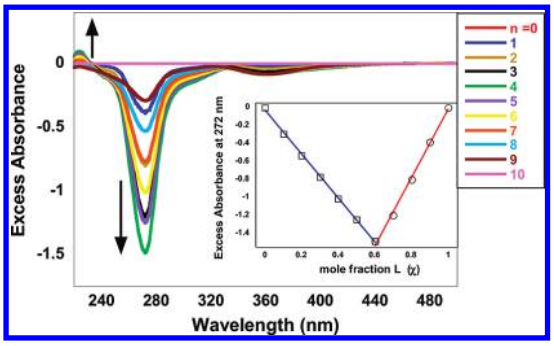

Figure 5. Job analysis of FerriCast with $Fe(ClO_4)_3$ in CH_3CN. The difference spectra represent iterations $n = 0$ to $n = 10$.

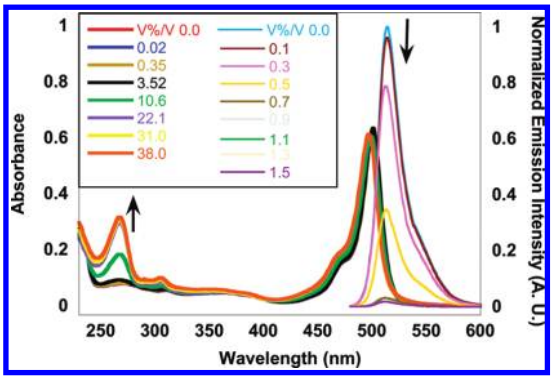

Figure 6. Methanolysis of $[Fe(\mathbf{3})_2]^{3+}$ in CH_3CN (25 μM **3**, 12.5 μM $Fe(ClO_4)_3$). The arrow indicates restoration of the apo-**3** band at 266 nm upon addition of MeOH (bold lines on the left). Decomplexation of 25 μM $[Fe(\mathbf{3})_2]^{3+}$ in CH_3CN with MES buffer (10 mM, pH = 5.8). The arrow indicates erosion of the emission intensity (λ_{ex} = 470 nm, λ_{em} = 514 nm) upon addition of buffer (thin lines on the right). Similar absorbance changes and losses of emission intensity are observed with other solvent titrants.

accounts for only a minor component (< 2%) of the iron complexes in solution. Counter ion effects are one possible explanation for the observed solution behavior and the anomalous Job analysis. Despite the difference in complexation between anions, FerriCast also does not bind $FeCl_3$ in aqueous solution.

Since FerriCast exhibited counterion dependent stoichiometry and no Fe^{3+} binding in aqueous solution, we prepared the fluorescent sensor **3** as an independent test of the coordination chemistry of $AT_2$12C4. Fe^{3+}-complexation of **3** was evaluated in aqueous solution by UV−vis spectroscopy, but no evidence of binding was observed. When the Fe^{3+}-binding of properties of **3** were interrogated by UV−vis spectroscopy in CH_3CN, the stoichiometry with $FeCl_3$ and $Fe(ClO_4)_3$ was identical to FerriCast. The binding constants of $\log\beta_{12} = 12.1$ with ClO_4, and $\log\beta_{11} = 5.2$ and $\log\beta_{12} = 8.0$ for Cl^- as the counterion. When the binding of $FeCl_3$ to **3** is evaluated by fluorescence as previously reported, however, the data fits a 1:1 isotherm with $\log\beta_{11} = 4.7$, a model that is also consistent with the Hill analysis of the data (coefficient = 1.1).[29] These results suggest the possibility of a species that is observable by absorption spectroscopy that does not significantly contribute to the emission behavior, possibly because it is only present at very low concentrations as predicted by simulation with Hyss. A variety of analytical techniques were screened to further interrogate the nature of the Fe^{3+} complexes of FerriCast and **3** in solution; however, none provided unambiguous corroborating evidence for any complex formulation. The observed speciation could be attributed to chloride acting as a coordinating ligand, inhibiting the formation of the 2:1 complex observed with perchlorate.

To assess the aqueous coordination chemistry of $AT_2$12C4, the Fe^{3+} complexes of FerriCast and **3** were formed in CH_3CN and exposed to various oxygen-containing solvents. Solutions of $[Fe(FerriCast)_2](ClO_4)_3$ or $[Fe(\mathbf{3})_2](ClO_4)_3$ in CH_3CN were titrated with CH_3OH, H_2O, DMSO, and 10 mM MES buffer (100 mM KCl, pH = 5.8), and the extent of decomplexation was assessed by measuring the restoration of the absorption at 272 nm (Figures 6, 7A and 7B). The point where 50% of the complex is decomplexed (DC_{50}) is reported in percent volume (V/V) of the oxygen containing solvents. The complexes were least sensitive to the presence of CH_3OH ($DC_{50} \sim 15\%$) and most sensitive to MES buffer ($DC_{50} \sim$ 0.5%, Figure 6). Identical trends were observed in the DC_{50} when $FeCl_3$ was used to perform the assay. The instability of the complex is consistent with Fe^{3+} coordination chemistry since it is a hard Lewis acid and an oxophilic metal ion.

These results are in contrast to previous reports on **3**, which suggests that Fe^{3+} induces an emission increase in aqueous solution (10 mM MOPS, pH = 5.1; or 10 mM TRIS/HCl, pH = 5.8).[5] The pH dependent emission behavior of **3** was not evaluated however. The current studies demonstrate that acidic media clearly facilitates the decomplexation of $[Fe(\mathbf{3})_2]^{3+}$ and $[Fe(FerriCast)]^{3+}$. Protonation of the aniline nitrogen atom of **3** also interrupts the PeT between the macrocyclic receptor and the fluorophore. When titrated with HCl, the magnitude of the fluorescence response of **3** is nearly identical to the response with $FeCl_3$. The conditional $pK_a' = 3.01$, as measured by fluorescence, was performed in 50% aqueous EtOH. When measured in 10% EtOH/water, the $pK_a' = 2.95$, nearly identical to the value measured in 50% aqueous EtOH. As a comparison to the fluorescent probe, $AT_2$12C4 was titrated in 50% aqueous EtOH with HCl, and a conditional $pK_a' = 3.92 \pm 0.01$ was measured. These values are consistent with reported pK_a's of other aniline derivatives.[30−34] The previous report on **3** describes using MOPS and TRIS at the extreme limit of their buffering capacities (MOPS 6.2−8.2 and TRIS 7.1−9.1), so the fluorescence enhancement observed in aqueous solution may have been misleading. Fe^{3+} rapidly hydrolyzes to various metal hydroxide species even under slightly acidic conditions (pH ∼ 5), so the enhanced emission likely results from sensor protonation upon metal hydrolysis. When titrated with 10 mM H_3PO_4/$H_2PO_4^-$ buffer (pH = 2.2), the measured fluorescence

(29) Dahlquist, F. W. *Methods Enzymol.* **1978**, *48*, 270–299.

(30) Lide, D. R. *CRC Handbook of Chemistry and Physics*, 83rd ed.; CRC Press: Boca Raton, FL, 2002; p 2664.
(31) Shen, Z.; Roehr, H.; Rurack, K.; Uno, H.; Spieles, M.; Schulz, B.; Reck, G.; Ono, N. *Chem.—Eur. J.* **2004**, *10*, 4853–4871.
(32) Maus, M.; Rurack, K. *New J. Chem.* **2000**, *24*, 677–686.
(33) Rurack, K.; Kollmannsberger, M.; Daub, J. *New J. Chem.* **2001**, *25*, 289–292.
(34) Descalzo, A. B.; Xu, H.-J.; Xue, Z.-L.; Hoffmann, K.; Shen, Z.; Weller, M. G.; You, X.-Z.; Rurack, K. *Org. Lett.* **2008**, *10*, 1581–1584.

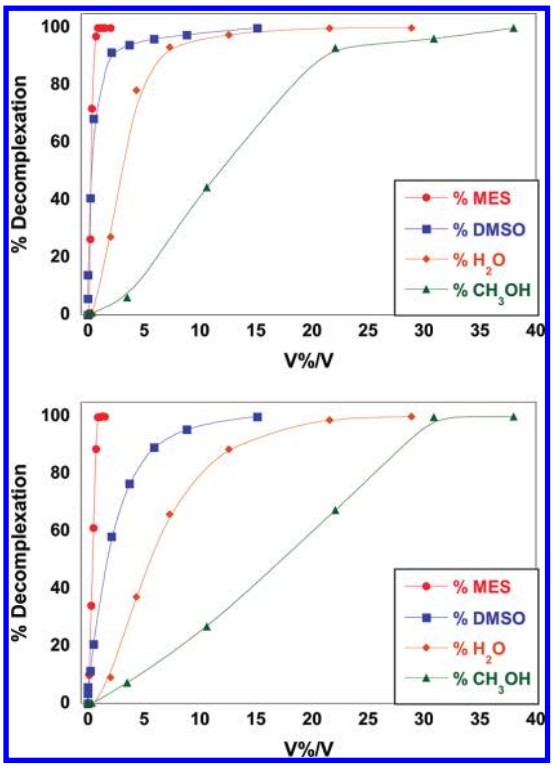

Figure 7. (A, top) Decomplexation of 25 μM $[Fe(FerriCast)_2]^{3+}$ in CH_3CN by various oxygen-containing solvents. (B, bottom) Decomplexation of 25 μM $[Fe(\mathbf{3})_2]^{3+}$ in CH_3CN by various oxygen-containing solvents.

intensity of **3** in CH_3CN remained constant in contrast to the titration with MES (pH = 5.8) where the emission intensity decreases rapidly. With the MES titration, however, the background fluorescence is greater than apo-sensor in CH_3CN, which suggests **3** is partially protonated.

The metal binding chemistry of Zn^{2+}, Ga^{3+}, and Cu^{2+} with the FerriCast model ligand $AT_2$12C4 also was screened to provide possible insight into the Fe^{3+} binding chemistry. Both Zn^{2+} and Ga^{3+} are closed shell metal ions that form complexes lacking CT bands that could complicate the fitting of spectrophotometric data. Ga^{3+} is a well-known diamagnetic structural analogue of Fe^{3+}. Job analysis of $AT_2$12C4 in CH_3CN with $Zn(ClO_4)_2$ reveals the presence of a 1:1 complex, but the weak association constant of this complex (log K_{11} = 3.1 ± 0.1) precludes the possibility of observing an even lower affinity 2:1 complex. When $AT_2$12C4 was titrated with $GaCl_3$ in CH_3CN, a 1:1 complex with a log K_{11} = 6.2 ± 0.3 was observed; however, Job analysis demonstrated ambiguous speciation similar to $FeCl_3$. The $GaCl_3$ $AT_2$12C4 data is consistent with the interactions observed between FerriCast and $FeCl_3$, but $Ga(ClO_4)_3$ is not readily available for making analogous measurements to $Fe(ClO_4)_3$. Additional attempts to observe and study these metal complexes by NMR and mass spectroscopy were not informative.

Structural Studies and Redox Chemistry. Repeated attempts to crystallize the Fe^{3+} complex of $AT_2$12C4 in diverse conditions with a variety of anions (Cl^-, BF_4^-, BPh_4^-, ClO_4^-, NO_3^-, etc.) were unsuccessful. Insoluble powders formed readily, even under dilute conditions.

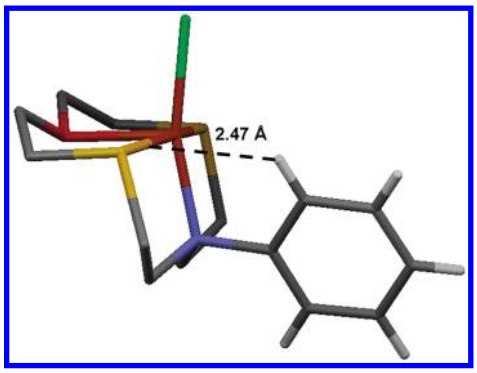

Figure 8. Bifurcated hydrogen bond in FerriCast model complex $[Cu(AT_2$12C4)Cl$](CuCl_2)$. The H-bond is shared between the Cu center and the bound thioether.

Alternatively, X-ray quality crystals of $[Cu(AT_2$12C4)-Cl$](CuCl_2)$ were obtained from an Et_2O diffusion into CH_3CN (Figure 2). The geometry of the metal complex initially appears to be square pyramidal; however, the short 2.47 Å distance between the Cu(1)−C(10) suggests the presence of a bifurcated hydrogen bond between the metal center and pendant H (Figure 8), which would make the geometry octahedral. The bifurcated hydrogen bond is shared between the copper and thioether of the macrocycle and is similar to a copper interaction in a previously reported crystal structure[35] that has been interrogated theoretically.[36] Despite this interesting solid state structural feature, it is unlikely that such an interaction is significant in solution.

Two additional types of crystals with different unit cells were isolated from the same setup, but neither diffracted well enough for additional structural analysis. This observation along with the presence of Cu^+ in the $CuCl_2^-$ counteranion in the complex indicates a redox process occurs over the course of the crystallization experiment. Cu^{2+} in CH_3CN induces homocoupling of dimethylaniline that proceeds through a radical cation intermediate (Scheme 2).[37] The putative oxidized aniline has a distinctive spectroscopic signature. When $AT_2$12C4 was treated with $Cu(ClO_4)_2$ in CH_3CN the fleeting radical cation $AT_2$12C4$^{\cdot+}$ can be observed at 455 nm before the product benzidine begins to appear at 352 nm (Figure 9). In addition to these features, the benzidine radical cation $(AT_2$12C4$)_2^{\cdot+}$ can also be observed at 956 nm. When Cu^{2+} is added to FerriCast or **3**, ligand oxidation can be observed spectrophotometrically and reduced copper can be detected with the Cu^+ indicator neocuprine. Although Fe^{3+}-induced oxidation of $AT_2$12C4, FerriCast and **3** is slow, a minor amount of background oxidation can be detected. While the UV−vis data suggest 1:1 M/L complex is the dominant species detected in $FeCl_3$ titrations with FerriCast and **3**, redox between the aniline-based $AT_2$12C4 receptor may account for some of the difficulties in fitting the data to an idealized model. While the data for $Fe(ClO_4)_3$ gives clear evidence for higher order speciation, a minor amount of 2:1 complex and/or ligand oxidation may occur in the $FeCl_3$ experiments.

(35) Castro, M.; Cruz, J.; Lopez-Sandoval, H.; Barba-Behrens, N. *Chem. Commun.* **2005**, 3779–3781.
(36) Thakur, T. S.; Desiraju, G. R. *Chem. Commun.* **2006**, 552–554.
(37) Kirchgessner, M.; Sreenath, K.; Gopidas, K. R. *J. Org. Chem.* **2006**, *71*, 9849–9852.

Scheme 2. Redox Chemistry between $AT_2$12C4 and Cu^{2+}

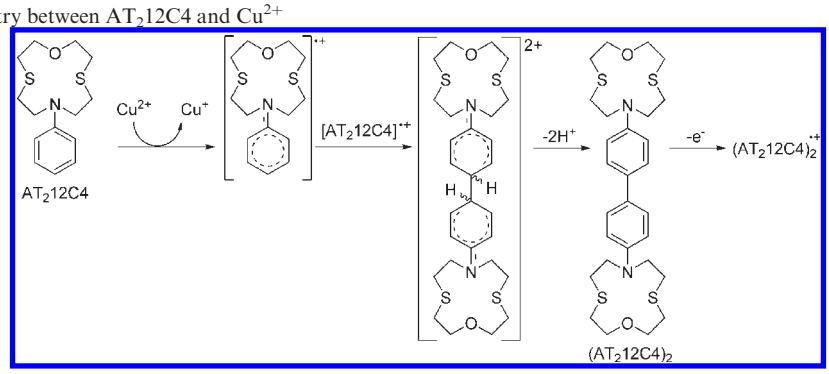

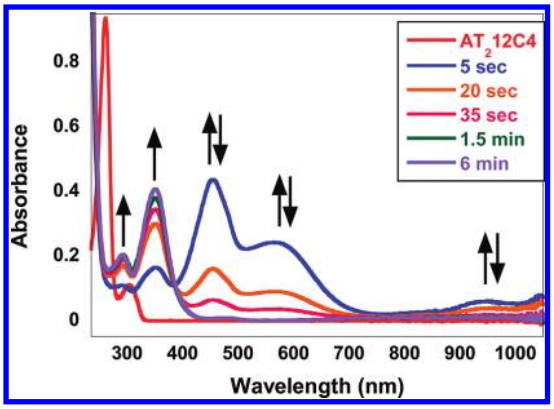

Figure 9. Redox reaction between $AT_2$12C4 and $Cu(ClO_4)_2$ in CH_3CN. The double headed arrows indicate the rapid growth and deterioration of electronic transitions that belong to the radical cation $AT_2$12C4$^{\bullet+}$ (455 nm) and radical cation of the resulting benzidine $(AT_2$12C4$)_2^{\bullet+}$ (956 nm). The single headed arrows indicate the formation of benzidine (352 nm).

Conclusions

In conclusion, we have prepared the new ferric iron cage FerriCast from a two step reaction sequence with improved yields over traditional methods. FerriCast behaves like a typical nitrobenzhydrol caged complex in CH_3CN; however, exposure of metalated FerriCast to solvents containing oxygen donors leads to decomplexation, which can be enhanced by ligand protonation. These results suggest that while $AT_2$12C4 possesses unique selectivity for Fe^{3+}, its application is limited to ones in nonaqueous solvents that lack strong oxygen donor atoms. In addition to the poor binding strength in aqueous media there is also the potential for redox chemistry with open-shell d-metals, which limits the utility of $AT_2$12C4 derived sensors and cages. A large number of fluorescent sensors contain aniline-based ligands and fluorophores, so it is important to consider redox chemistry in the mechanism of action, especially when using Cu^{2+} in CH_3CN. While the original report on **3** provides a compelling example of ligand design and fluorescence enhancement and Fe^{3+} enhanced fluorescence in CH_3CN, the fluorescence results in aqueous solution are inconsistent with the coordination chemistry of ligands containing $AT_2$12C4 macrocycles.

Acknowledgment. We thank Professor Christoph Fahrni for insightful discussion on the redox chemistry of anilines, and Professor Christopher Chang for helpful discussions. This work was supported by the University of Connecticut.

Supporting Information Available: ^1H and ^{13}C NMR spectra for compounds synthesized. Job analysis of **3** with $Fe(ClO_4)_3$. Titration data for FerriCast and **3** with $FeCl_3$ and $Fe(ClO_4)_3$. Hill analysis of fluorometric titration of **3** with $FeCl_3$. Decomplexation data for FerriCast and **3**. Titration data of FerriUnc with $FeCl_3$. Ferrioxalate actinometry and photolysis data for FerriCast. Titration data for $AT_2$12C4 with HCl, $Zn(ClO_4)_2$ and $GaCl_3$. Job plot of $AT_2$12C4 with $Zn(ClO_4)_2$. Fluorometric titration data for **3** with HCl. Spectroscopic data for the oxidation of FerriCast with $Cu(ClO_4)_2$. This material is available free of charge via the Internet at http://pubs.acs.org.